**Acta Cryst**

# STRUCTURAL
# CHEMISTRY

**Supporting information for article:**

## Synthesis, structure, antiproliferative and optical activities of two new biphenyl-derived Schiff bases

Xue-Jie Tan, Ling-Yao Zhang, Yuan-Kai Sun and Xue-Min Zhou

# Supporting information

**The explanations for the emission spectra of the title compounds.**

For the fluorescence spectra of **3-BEHMI**, four functionals render the same relative intensity ratio predication of the two bands, i.e. the intense peak has lower energy while the weak peak has higher energy (Figs S13-S16), which is exactly reverse with experimental results (Fig. 6b). On the point of band maximum positions of the simulated spectra, the most reliable result is that performed with B3LYP (Fig. S13). The emission wavelengths in ethanol solution are 338 and 440 nm; the wavelengths in the gas phase are 335 and 432 nm, both fall into the experimental scopes (310-340 nm and 400-450 nm). However, the emission energies using other functionals are quite different and significantly worse. Sometimes the reliable result is obtained only in the gas phase (PBE1PBE, Fig. S15); and sometimes considering solvent effects may result in better simulations (M062X and WB97XD, Fig. S14 and S16) than that in the gas phase, yet only one band is reliable. At last, the results from TD-DFT/B3LYP/PCM approach were used for MO analysis.

**3-BEHEI** shows one strong fluorescence band between 310-350 nm, upon excitation at 200, 220 and 280 nm (Fig. 7b). None of the calculated emission spectra represent a good approximation (Figs S17-S20). The influences of the functionals and the solvent corrections on the calculated emission energies are rather dramatic. For different functionals, the deviations may exceed 58 nm (M062X and PBE1PBE in PCM); for solvent affection, the deviations may exceed 57 nm (PBE1PBE method in the gas phase and ethanol solution). In order to get a more reliable simulation, we have considered two more approaches to calculate the fluorescence of **3-BEHEI**, i.e. TD-DFT/B3P86 (Becke, 1996; Becke, 1993; Becke, 1988; Perdew, 1986) and configuration interaction single (CIS) approach (Foresman *et al.*, 1992). The results are listed in Figs. S21 and S22. Apparently, both of them work poorly. So, no MO analysis was performed on the fluorescence of **3-BEHEI**.

Becke, A. D. (1996). *J. Chem. Phys.* **104**, 1040–1046.

Becke, A. D. (1993). *J. Chem. Phys*. **98**, 5648–5652.

Becke, A. D. (1988). *Phys. Rev.* A**38**, 3098–3100.

Foresman, J. B., Head-Gordon, M., Pople, J.A. & Frisch, M.J. (1992). *J. Phys. Chem*. **96**, 135–149.

Perdew, J. P. (1986). *Phys. Rev.* B **33**, 8822–8824.

**Table S1** Comparison of experimental and calculated UV-Vis characteristic peaks and predicted transitions.

| molecules | $\lambda_{max}$ ($\varepsilon$) [i] | $\lambda$ ($f$) | MO transitions (configurations) [v] |
|---|---|---|---|
| | | | H-2->L+10(+11%)  H-2->L+2(+10%) |
| | 203.0 ($1.2\times10^5$) [ii] | 191.9 (0.3618) [iii] | H-1->L+1(+8%)  H-2->L+14(+6%) |
| | | | H-2->L+9(+6%)  H-2->L+1(+5%) |
| | | | H-4->L+0(+17%)  H-0->L+8(15%) |
| | 222.0 ($0.8\times10^5$) [ii] | 208.4 (0.1614) [iii] | H-0->L+6(11%)  H-1->L+3(9%) |
| **3-BEHMI** | | | H-0->L+5(6%)  H-1->L+5(+6%) |
| | | | H-5->L+0(+5%)  H-0->L+3(+5%) |
| | | 265.6 (0.0967) [iii] | H-0->L+1(+56%)  H-1->L+0(+22%) |
| | | | H-0->L+2(6%) |
| | 282.0 ($0.4\times10^5$) [ii] | 257.5 (0.0972) [iii] | H-1->L+0(+40%)  H-0->L+2(+20%) |
| | | | H-2->L+1(+10%)  H-2->L+0(+9%) |
| | 348.0 ($0.8\times10^5$) [ii] | 328.8 (1.7285) [iii] | H-0->L+0(+87%) |
| | 204.0 ($1.8\times10^5$) [ii] | 191.8(0.3184) [iv] | H-1->L+5(+15%)  H-6->L+2(7%) |
| **3-BEHEI** | | | H-0->L+12(+6%) |
| | 301.0 ($1.1\times10^5$) [ii] | 301.6 (1.2561) [iv] | H-1->L+0(+42%)  H-0->L+0(36%) |

[i]: wavelength in nm, molar extinction coefficients in $L \cdot mol^{-1} \cdot cm^{-1}$.

[ii]: the solvent is ethanol.

[iii]: calculated using the TD-DFT/M062X/6-311+G(d,p) method in ethanol solution (PCM).

[iv]: calculated using the TD-DFT/WB97XD/6-311+G(d,p) method in ethanol solution (PCM).

[v]: contour plots and energies of frontier molecular orbitals see **Figs. S23 – S24.**

**Table S2** Comparison of experimental and calculated fluorescence characteristic peaks and predicted transitions.

| molecule | $\lambda_{max}$ [i] | $\lambda$ ($f$) [ii] | MO transitions (configurations) [iii] |
|---|---|---|---|
| | | | L->H-2 (54%) |
| **3-BEHMI** | 310-340 | 337.6 (0.0663) | L->H-3 (39%) |
| | | | L+1->H-1 (4%) |
| | 400-450 | 439.8 (1.6624) | L->H-1 (99%) |

[i]: wavelength in nm, the solvent is ethanol. The wavelength ranges instead of emission peaks are listed because the maximum positions differ depending on the wavelength of exciting light.

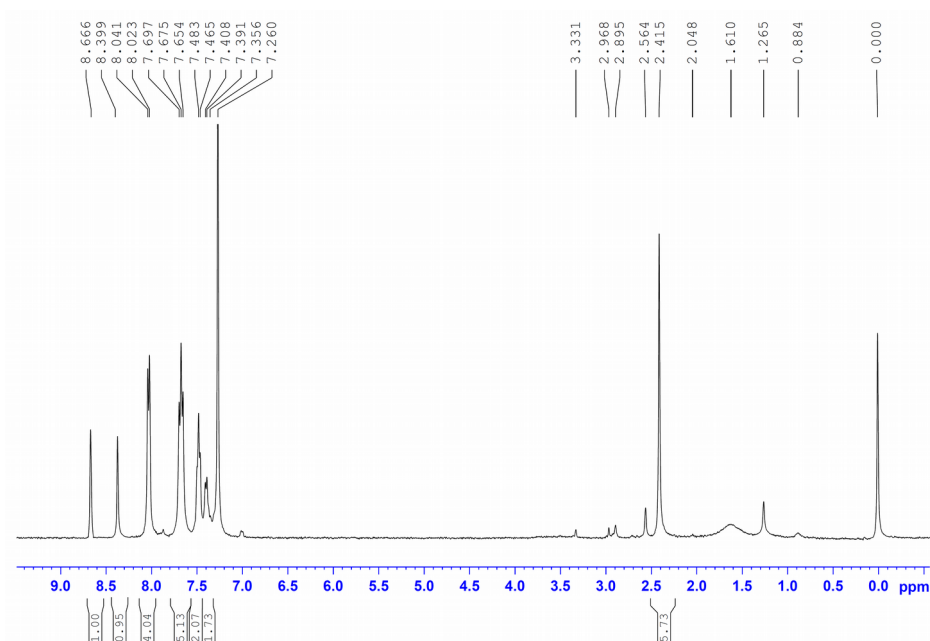[ii]: calculated using the TD-DFT/B3LYP/6-311+G(d,p) method in ethanol solution (PCM).

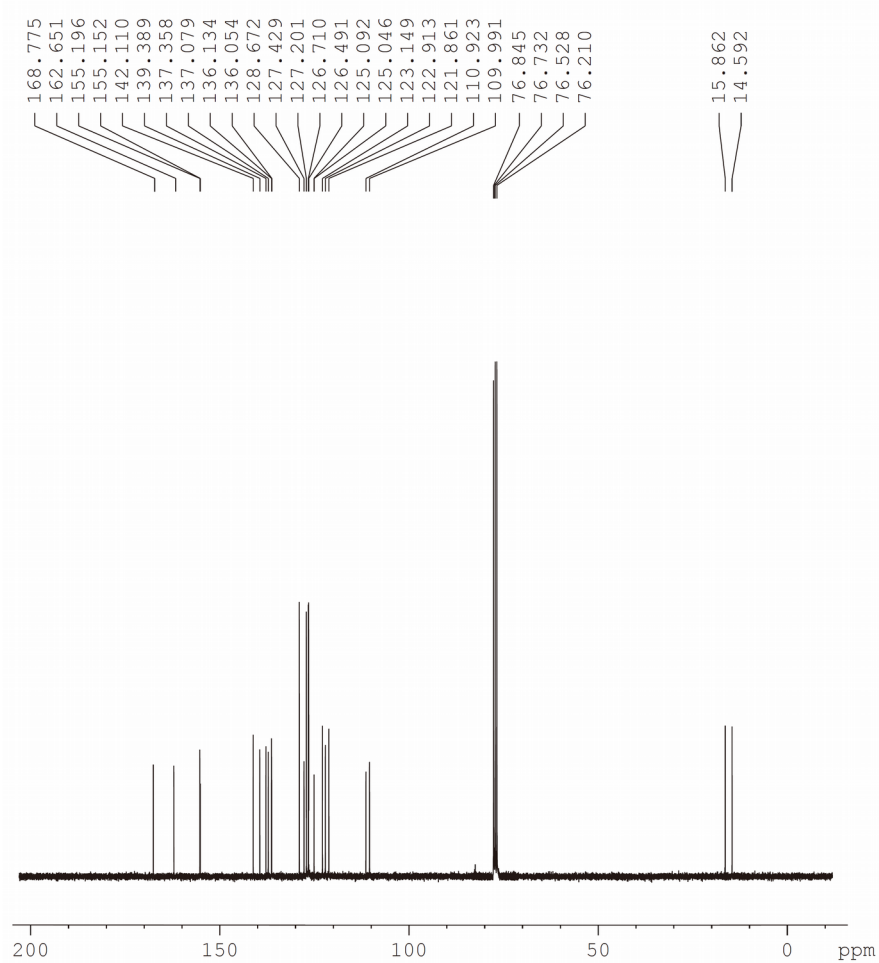[iii]: contour plots and energies of frontier molecular orbitals see **Fig. S25.**
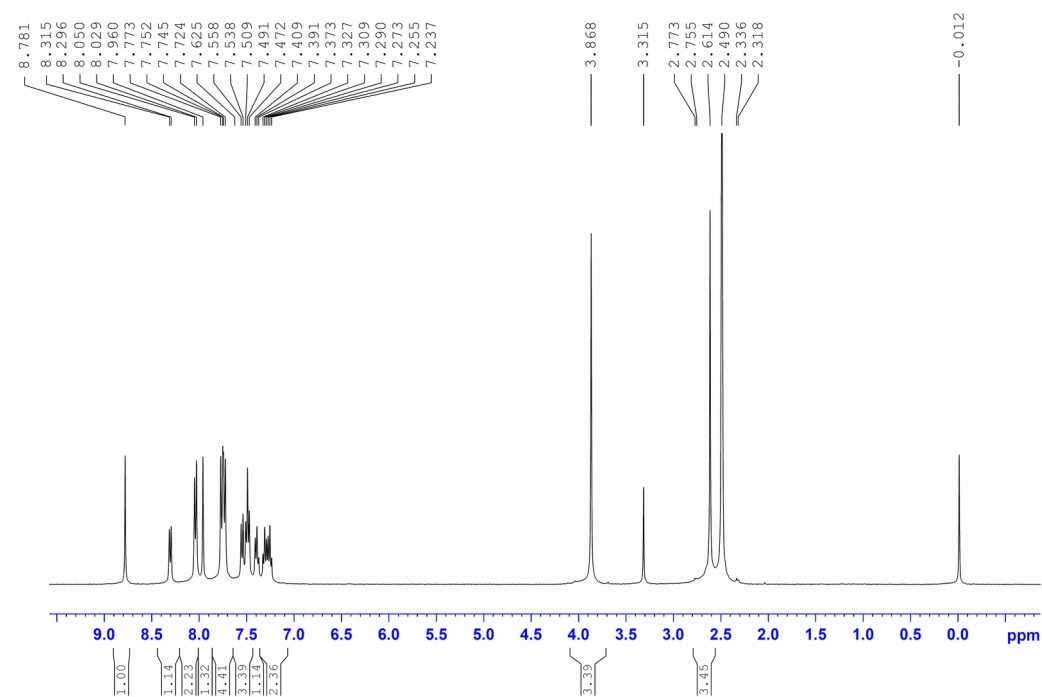
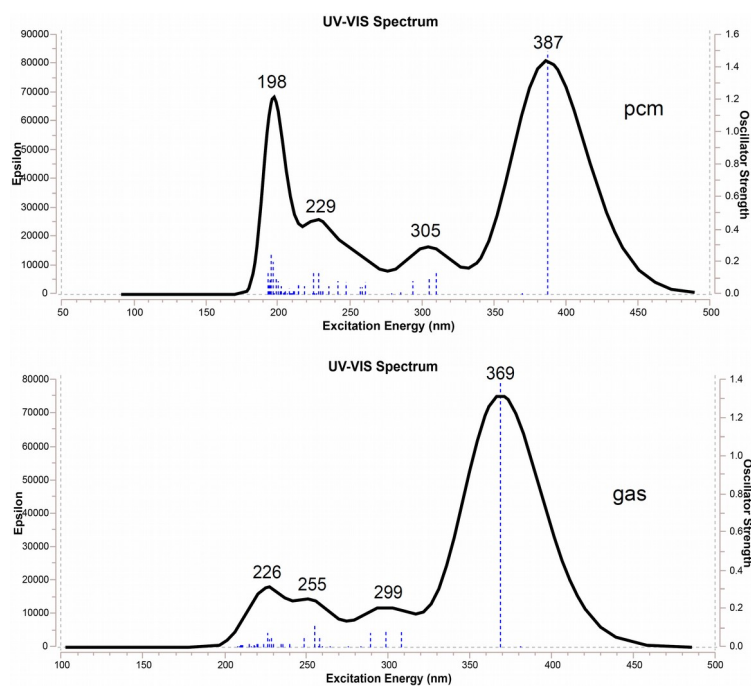**Figure S1**      ¹HNMR spectrum of **3-BEHMI** (in DMSO-d6).
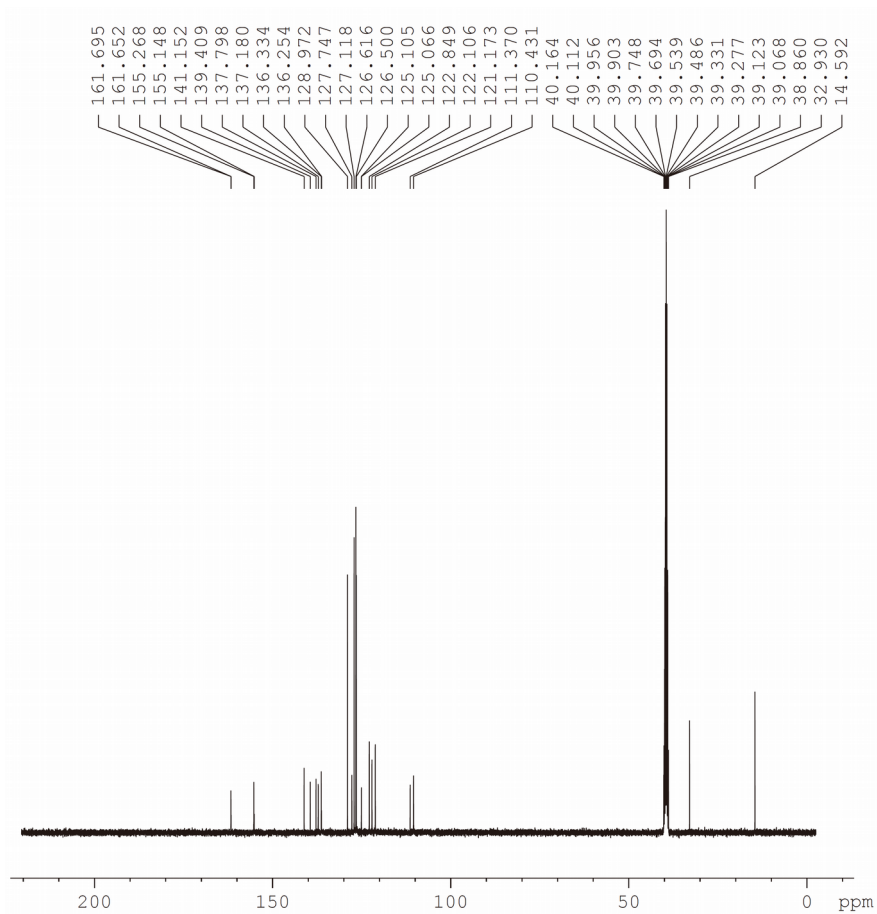


**Figure S2**      ¹³CNMR spectrum of **3-BEHMI** (in DMSO-d6).
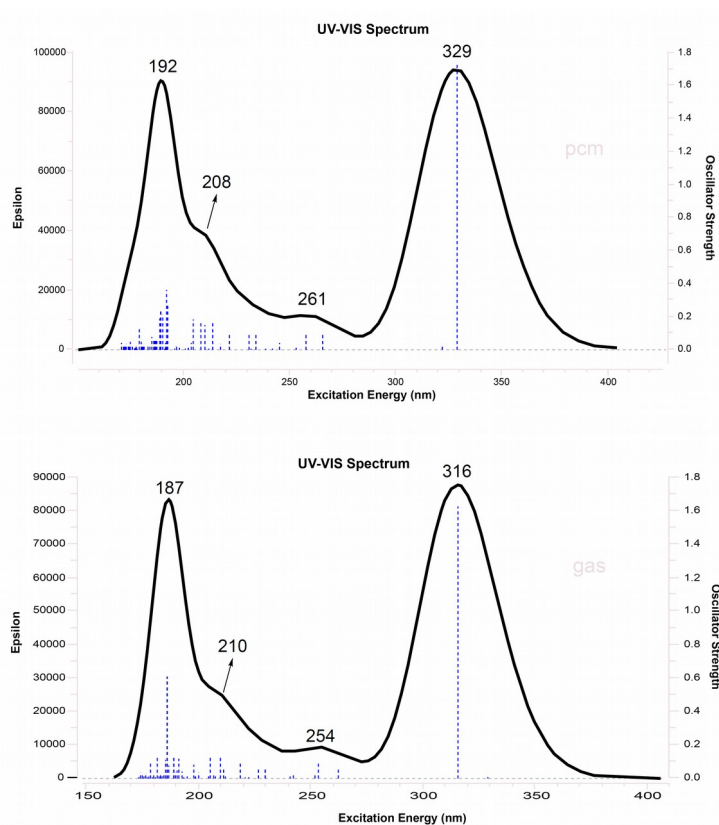
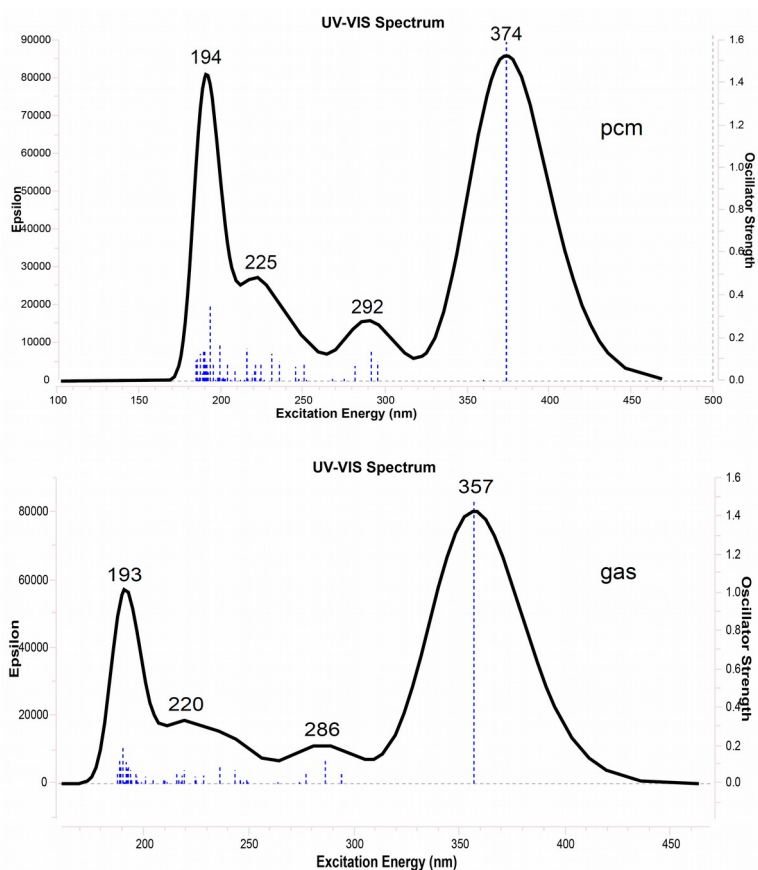**Figure S3**        ^{1}HNMR spectrum of **3-BEHEI** (in CDCl₃).



**Figure S4**        ^{13}CNMR spectrum of **3-BEHEI** (in CDCl₃).
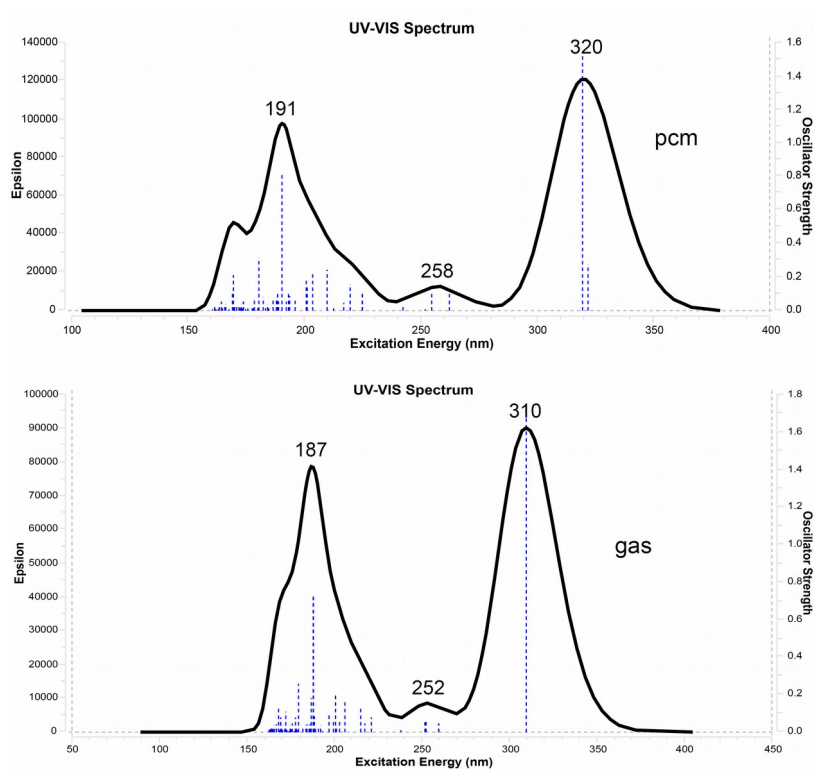
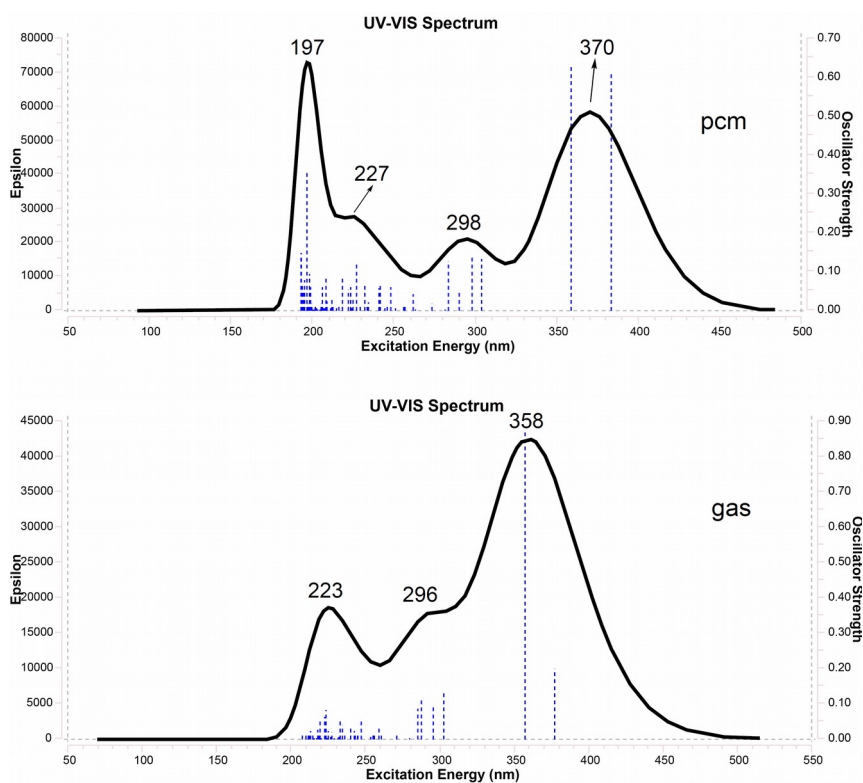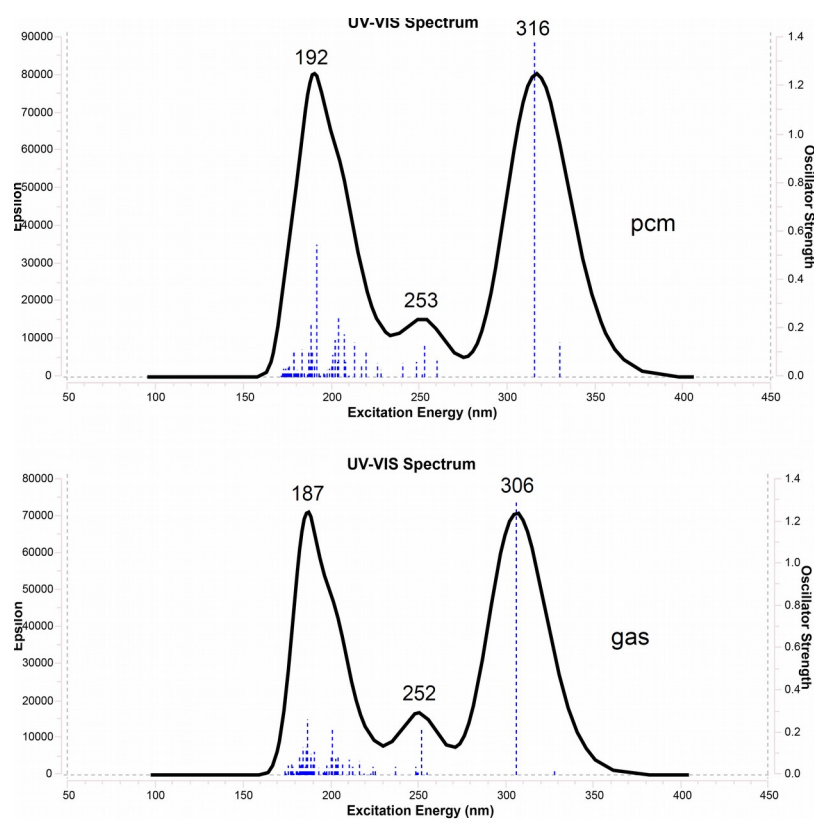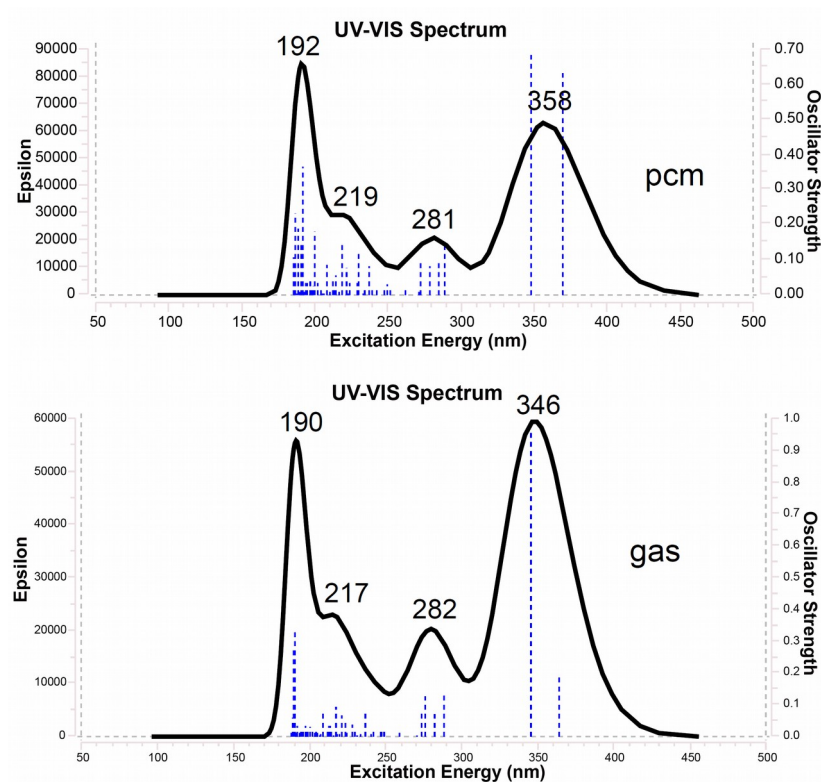**Figure S5**      calculated UV–Vis spectra of **3-BEHMI** with TD-DFT/B3LYP/6-311+G(d,p) method.
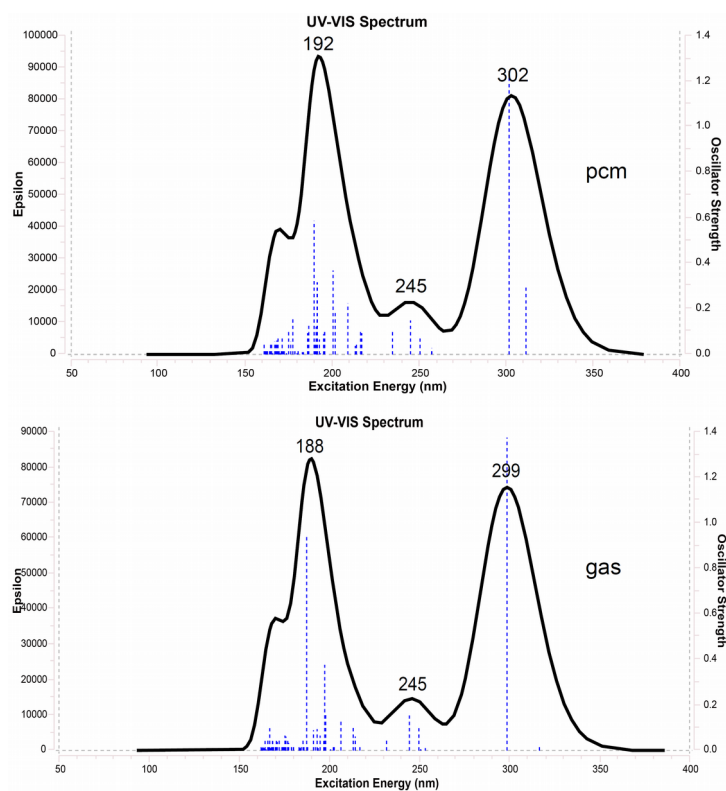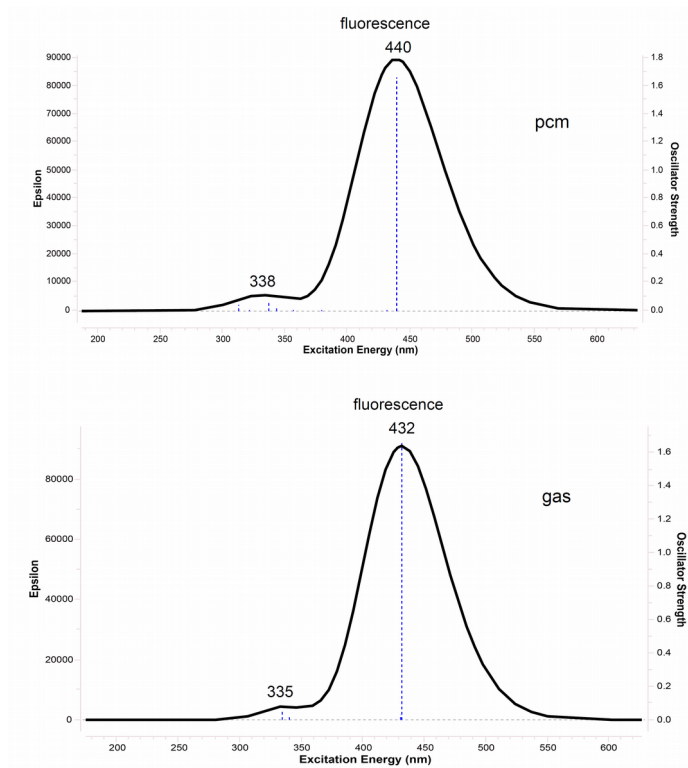


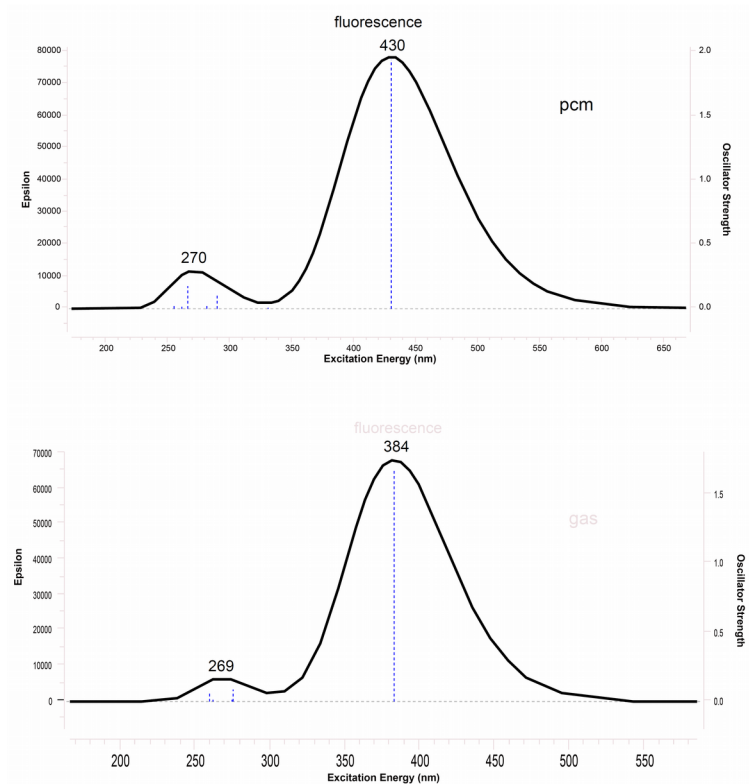**Figure S6**      calculated UV–Vis spectra of **3-BEHMI** with TD-DFT/M062X/6-311+G(d,p) method.

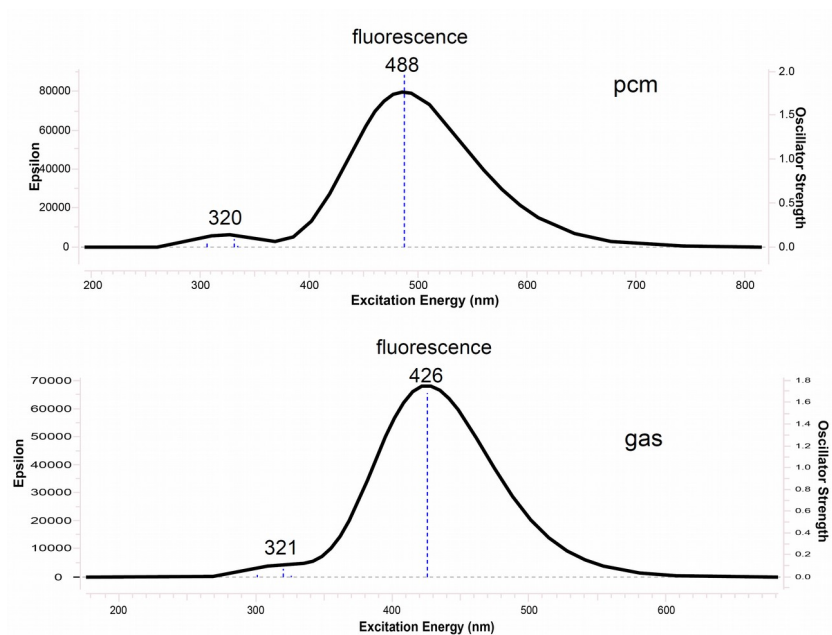**Figure S7**      calculated UV–Vis spectra of **3-BEHMI** with TD-DFT/PBE1PBE/6-311+G(d,p) method.

**Figure S8**    calculated UV–Vis spectra of **3-BEHMI** with TD-DFT/WB97XD/6-311+G(d,p) method.

**Figure S9**    calculated UV–Vis spectra of **3-BEHEI** with TD-DFT/B3LYP/6-311+G(d,p) method.

**Figure S10** calculated UV–Vis spectra of **3-BEHEI** with TD-DFT/M062X/6-311+G(d,p) method.



**Figure S11** calculated UV–Vis spectra of **3-BEHEI** with TD-DFT/PBE1PBE/6-311+G(d,p) method.

25

**Figure S12**    calculated UV–Vis spectra of **3-BEHEI** with TD-DFT/WB97XD/6-311+G(d,p) method.
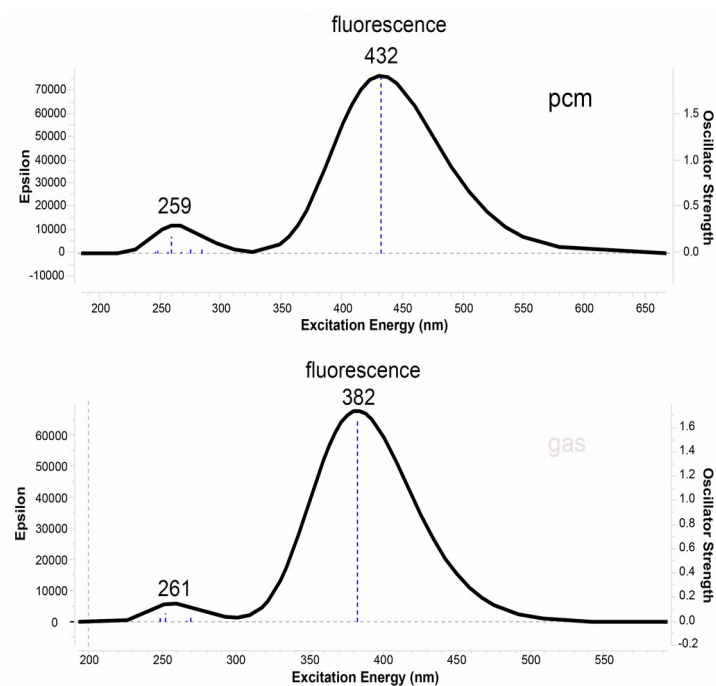


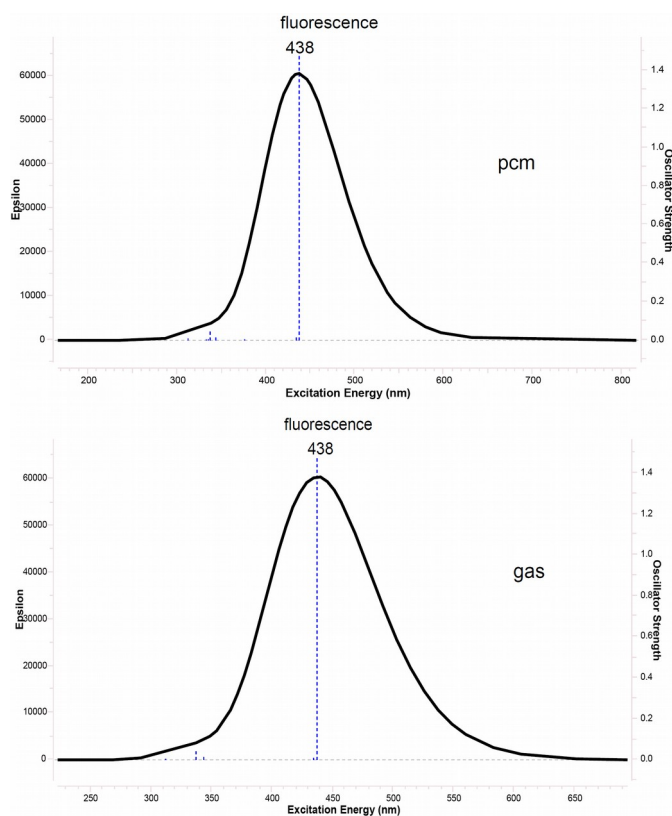**Figure S13**    calculated fluorescence spectra of **3-BEHMI** with TD-DFT/B3LYP/6-311+G(d,p) method.

**Figure S14**    calculated fluorescence spectra of **3-BEHMI** with TD-DFT/M062X/6-311+G(d,p) method.
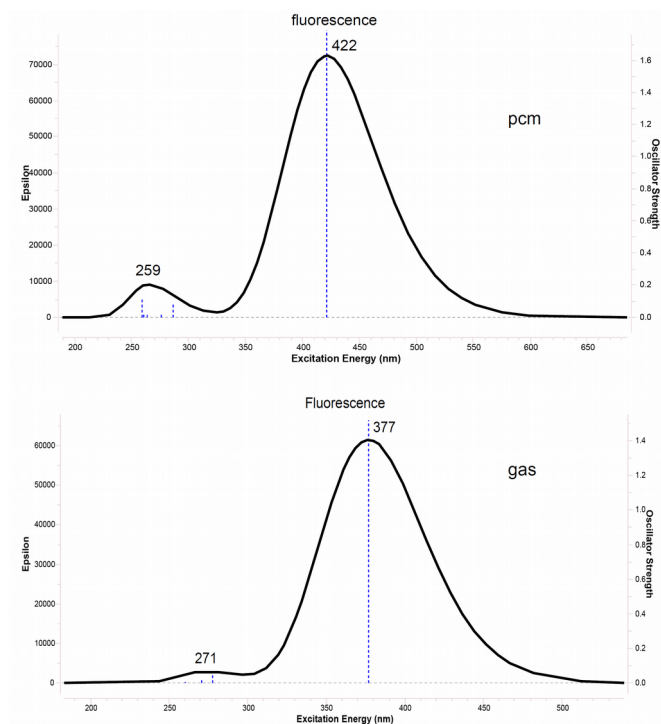


**Figure S15**    calculated fluorescence spectra of **3-BEHMI** with TD-DFT/PBE1PBE/6-311+G(d,p) method.
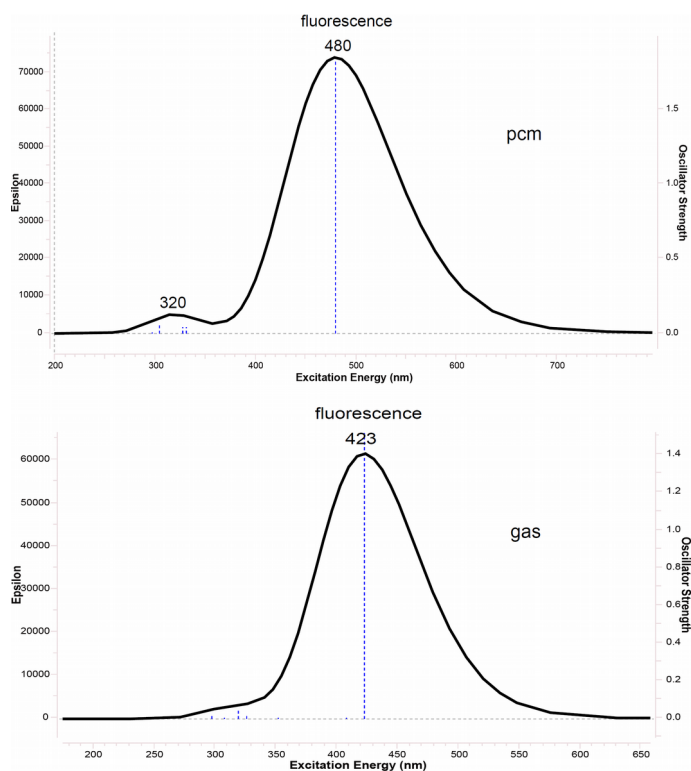
**Figure S16**   calculated fluorescence spectra of **3-BEHMI** with TD-DFT/WB97XD/6-311+G(d,p) method.
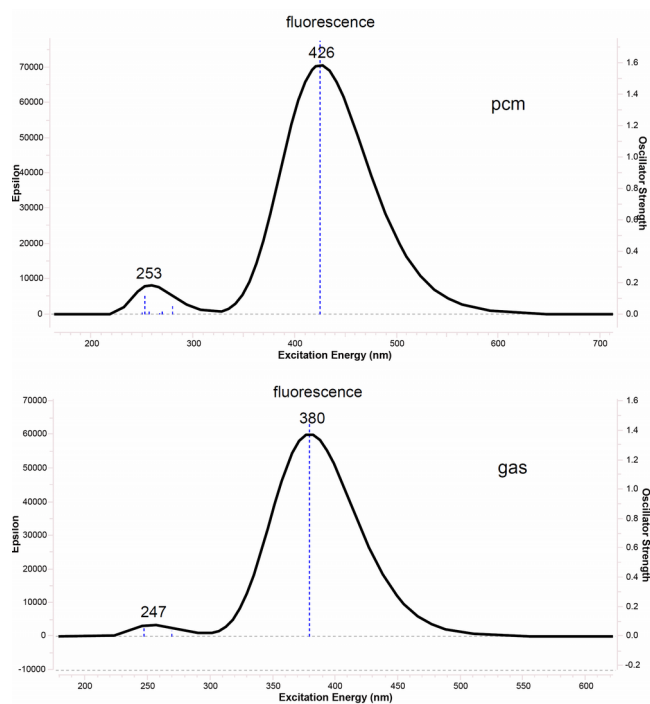


**Figure S17**   calculated fluorescence spectra of **3-BEHEI** with TD-DFT/B3LYP/6-311+G(d,p) method.
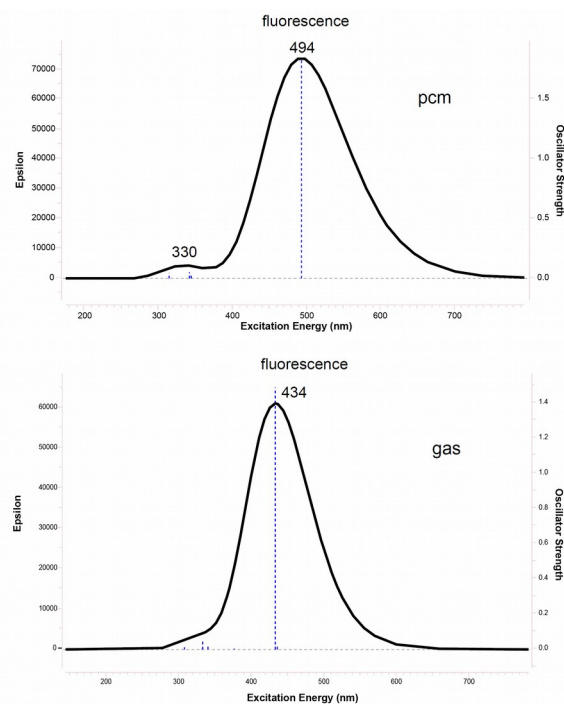
**Figure S18**    calculated fluorescence spectra of **3-BEHEI** with TD-DFT/M062X/6-311+G(d,p) method.
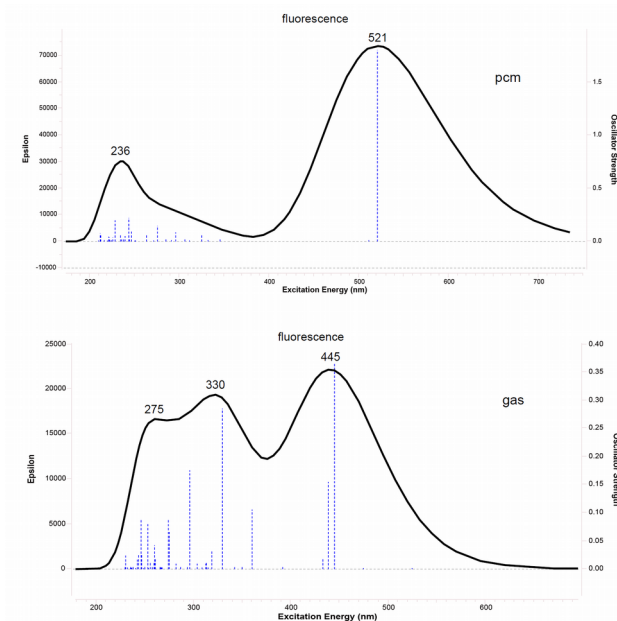


**Figure S19**    calculated fluorescence spectra of **3-BEHEI** with TD-DFT/PBE1PBE/6-311+G(d,p) method.
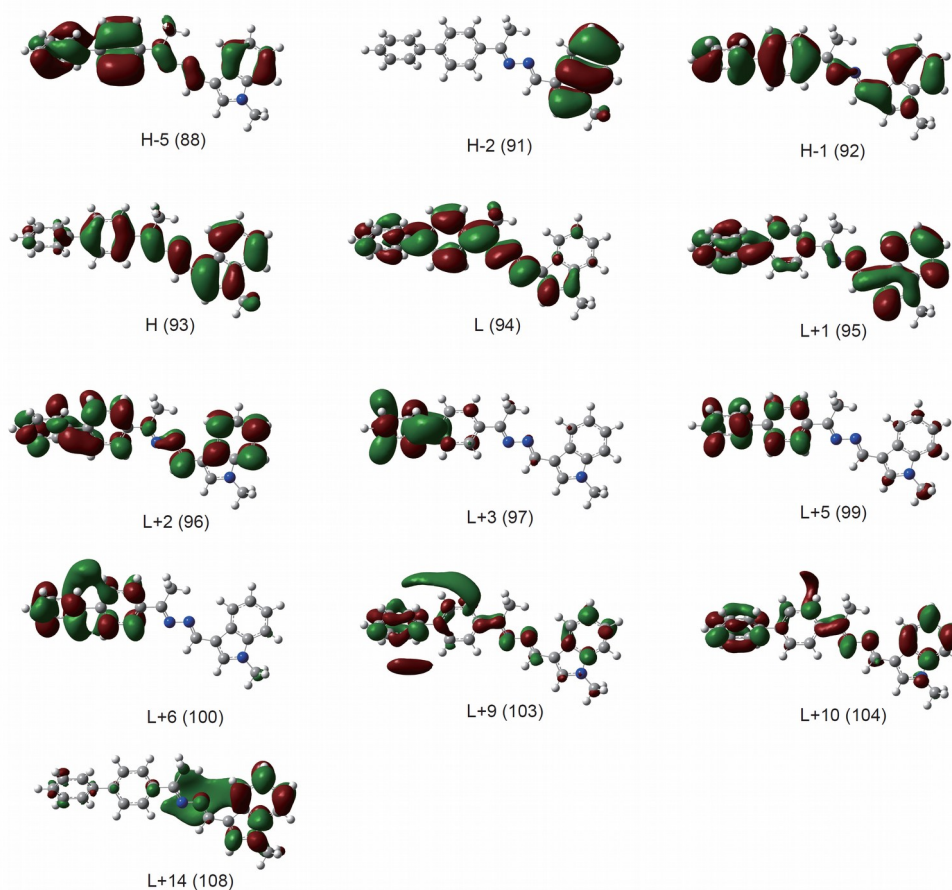
**Figure S20**    calculated fluorescence spectra of **3-BEHEI** with TD-DFT/ WB97XD /6-311+G(d,p) method.



**Figure S21**    calculated fluorescence spectra of **3-BEHEI** with TD-DFT/ B3P86/6-311+G(d,p) method.
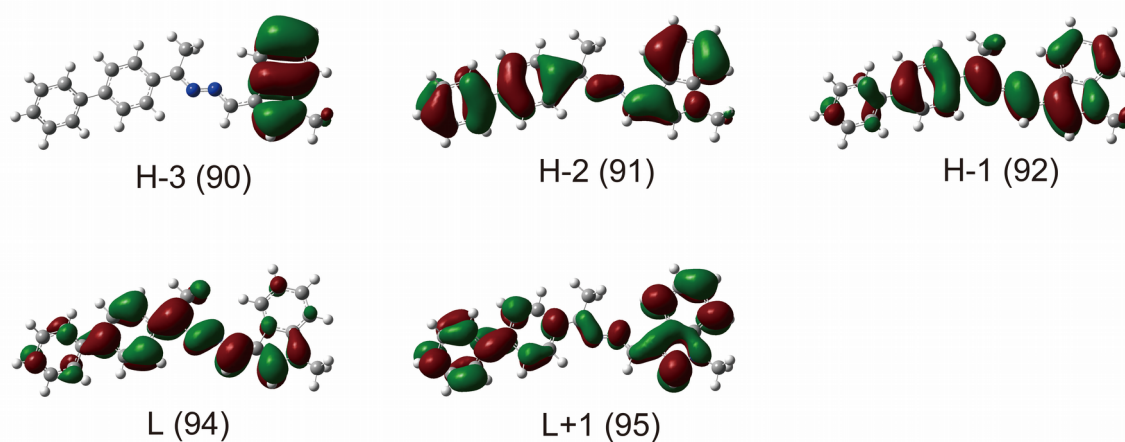
**Figure S22**      calculated fluorescence spectra of **3-BEHEI** with CIS/B3LYP/6-311+G(d,p) method.



**Figure S23**      Kohn−Sham ortibals relevant for transition at 191.9, 208.4, 305.3 and 387.3 nm in the simulated UV-Vis spectrum of **3-BEHMI** (Table S1), calculated using the TD-DFT/M062X/6-311+G(d,p) method in ethanol solution (PCM).

H-6 (87)   H-1 (92)   H (93)

L (94)   L+2 (96)   L+5 (99)

L+12 (106)
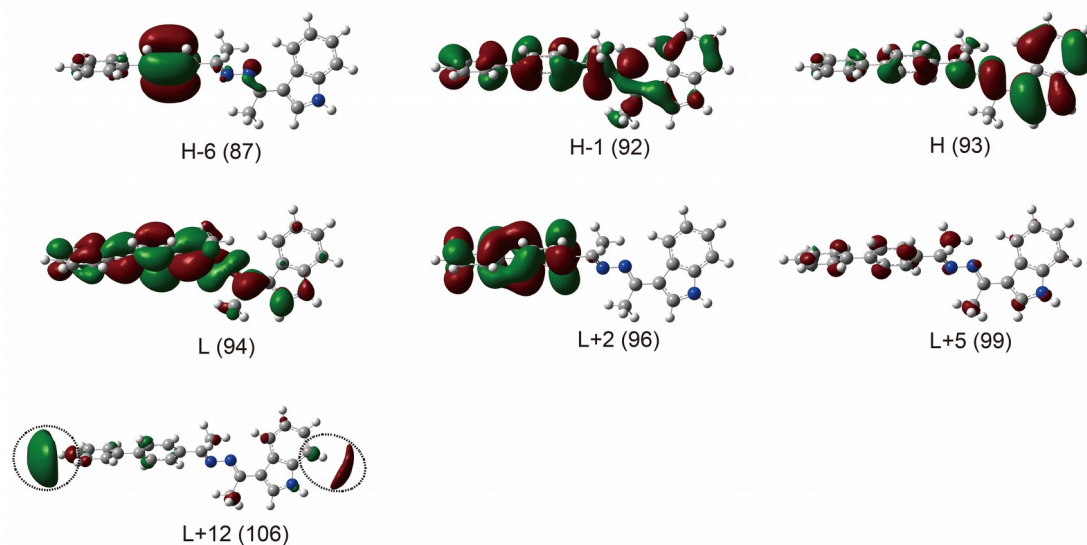
**Figure S24** Kohn−Sham ortibals relevant for transition at 191.8 and 301.6 nm in the simulated UV-Vis spectrum of **3-BEHEI** (Table S1), calculated using the TD-DFT/WB97XD/6-311+G(d,p) method in ethanol solution (PCM).



H-3 (90)   H-2 (91)   H-1 (92)

L (94)   L+1 (95)

**Figure S25** Kohn−Sham ortibals relevant for transition at 337.6 and 439.8 nm in the simulated fluorescence spectrum of **3-BEHMI** (Table S2), calculated using the TD-DFT/B3LYP/6-311+G(d,p) method in ethanol solution (PCM).